[21] Detachment, Surface Migration, and Other Dynamic Behavior in Bacterial Biofilms Revealed by Digital Time-Lapse Imaging

By PAUL STOODLEY, LUANNE HALL-STOODLEY, and HILARY M. LAPPIN-SCOTT

Introduction

Over the past decade much biofilm research has focused on the ultrastructural complexity of biofilms and the implications that the observed organization may have on biofilm processes.This interest was largely sparked by the development of confocal microscopy (CM), which allowed biofilms to be observed at high resolution in 3D with no disruption to structure.[1] These studies revealed that biofilms, both in the laboratory and in nature, are often heterogeneous and consist of microcolonies or cell clusters (aggregates of microbial cells in an extracellular polysaccharide slime matrix) separated by interstitial voids and channels.[2] Further, with the use of tracer particles[3] and microelectrodes,[4] it was found that the channels allowed water to flow around the biofilm structures. These channels, depending on the hydrodynamic conditions, could significantly increase the supply of nutrients to bacterial cells in the biofilm. Detailed descriptions of the principles and applications of CM to the imaging of biofilms can be found in Caldwell *et al.*[1] and Lawrence and Neu[5]. Evidence that biofilm structure may influence growth and activity, as well as the possibility that the structure may represent an optimal organizational arrangement for growth in a particular environment, has prompted increased interest in this area of biofilm research. Other microscopic techniques such as deconvolution microscopy[6] and differential interference contrast microscopy,[7] have also been used to image biofilm structure at high resolution.

Although much work has been done, and is currently being undertaken, to determine the spatial complexities of biofilm systems, the dynamic behavior in biofilms has been less well studied. Time lapse studies are generally limited to the tracking of individual cells attaching, moving over, and detaching from surfaces in the initial stages of biofilm formation.These studies have allowed the

[1] D. E. Caldwell, D. R. Korber, and J. Lawrence, *in* "Advances in Microbial Ecology," Vol. 12 (K. C. Marshall, ed.), p. 1. Plenum Press, New York, 1992.
[2] P. Stoodley, D. deBeer, J. D. Boyle, and H. M. Lappin-Scott, *Biofouling* **14**, 75 (1999).
[3] P. Stoodley, D. deBeer, and Z. Lewandowski, *Appl. Environ. Microbiol.* **60**, 2711 (1994).
[4] D. deBeer and P. Stoodley, *Water Sci. Tech.* **32**, 11 (1995).
[5] J. R. Lawrence and T. R. Neu, *Methods Enzymol.* **310**, 131 (1999).
[6] D. Phipps, G. Rodriguez, and H. Ridgway, *Methods Enzymol.* **310**, 178 (1999).
[7] J. Rogers and C. W. Keevil, *Appl. Environ. Microbiol.* **58**, 2326 (1992).

0076-6879/00 $35.00

direct measurement of the accumulation rate of cells on a surface[8] and given insight into the dynamic behavior of attached cells. Dalton *et al.*[9] and O'Toole and Kolter[10] have demonstrated that biofilm microcolonies can repeatedly form and disperse from the coordinated movement of single attached cells to specific loci on a surface. Without time lapse imaging it might be assumed that in these cases the microcolonies were generated from growth, not migration. However, it is much more difficult to keep track of single cells within mature, thick biofilms, since they are easily lost against a background of cells of similar appearance. This task is made more difficult if the biofilm cells are motile or "twitching." To overcome these problems we have used time lapse imaging at lower power magnification to reveal dynamic behavior in biofilms by tracking entire biofilm microcolonies rather than individual bacterial cells. These methods and some results that demonstrate the utility of these methods are presented in this paper.

Biofilm Reactor Systems, Flow Cells, and Digital Imaging

Two components are required to image the development and behavior of living biofilms in real time. First, a reactor system is required that incorporates flow cells (sometimes called perfusion chambers) that have a transparent wall or window for microscopic observation. Second, a microscope and imaging system are required to collect and manipulate digital images.

Reactor Systems

There are many types of flow cells, which are often designed and constructed "in house." Some of these have been described in detail elsewhere.[11–13] Some flow cells are also commercially available (BioSurface Technologies Corporation, Bozeman, MT, http://www.imt.net/~mitbst/flowcell.html). The flow cells are incorporated into a flow system that is generally either "once through" or "recirculating." In "once through" systems, which are the most commonly used in biofilm studies, sterile nutrients are pumped through the flow cell into a waste container at the effluent end.[12] In these setups the flow rate cannot be adjusted independently of

[8] A. Escher and W. G. Characklis, *in* "Biofilms" (W. G. Characklis and K. C. Marshall, eds.), p. 445. Wiley, New York, 1990.
[9] H. M. Dalton, A. E. Goodman, and K. C. Marshall, *J. Ind. Microbiol.* **17,** 228 (1996).
[10] G. A. O'Toole and R. Kolter, *Mol. Microbiol.* **30,** 295 (1998).
[11] L. Hall-Stoodley, J. C. Rayner, P. Stoodley, and H. M. Lappin-Scott, *in* "Methods in Biotechnology," Vol. 12: "Environmental Monitoring of Bacteria" (C. Edwards, ed.), p. 307. Humana Press, Totowa, NJ, 1999.
[12] R. J. Palmer, *Methods Enzymol.* **310,** 160 (1999).
[13] M. S. Zinn, R. D. Kirkegaard, R. J. Palmer, and D. C. White, *Methods Enzymol.* **310,** 224 (1999).

the residence time and the cost and time required to prepare sterile media usually limits experiments to low, laminar flows. In "recirculating" systems the flow cells are incorporated into a recirculating loop attached to a mixing chamber (Fig. 1). Sterile nutrients are added to the mixing chamber and the residence time (θ) can be controlled by the nutrient flow rate (Q_n) according to $\theta = V/Q_n$, where V is the volume of the mixing chamber *plus* the recirculation loop. These systems have the advantage that the flow rate in the flow cells can be adjusted independently of the nutrient flow rate so that much higher flow rates can be achieved in the flow cells without using impractical volumes of media. Also, the Q_n can be adjusted so that the dilution rate ($D = Q_n/V$) is greater than the specific growth rate of the organism being investigated so planktonic cells are continually "washed out" and only the attached biofilm population is retained.[14] Therefore, it can be assumed that any cells or microcolonies in the bulk liquid must have resulted from detachment and not planktonic growth. However, these systems have several disadvantages. First, they generally have large surface areas and there can be significant biofilm accumulation in areas other than those being observed in the flow cells (mixing chamber, connective tubing). Second, the biofilms in the flow cells are continually exposed to detached cells and waste products that build up to steady-state concentrations in the reactor system. A comprehensive mass balance analysis of various biofilm reactor systems may be found in Characklis.[14]

Image Capture, Enhancement, and Analysis

Digital microscopic image analysis requires four key components: a microscope, a digital camera, a computer with an installed framestore board, and software for capture, image enhancement, and analysis. Often the same software can be used for image capture and analysis. There are many different types of systems available with a variety of features and a range of prices. In this paper we describe the system found to be economical and relatively easy to operate.

Biofilm Reactor System for Growing Biofilms in Laminar or Turbulent Flow

For some experiments we wished to determine the influence of flow velocity on biofilm structure and behavior and required a flow system that could operate over a wide range of laminar and turbulent flows and in which the hydrodynamics were well characterized. To achieve this we designed a recirculating flow system based on a system previously described by Bryers and Characklis.[15] The reactor

[14] W. G. Characklis, *in* "Biofilms" (W. G. Characklis and K. C. Marshall, eds.), p. 17. Wiley, New York, 1990.

[15] J. D. Bryers and W. G. Characklis, *Water Res.* **15**, 483 (1981).

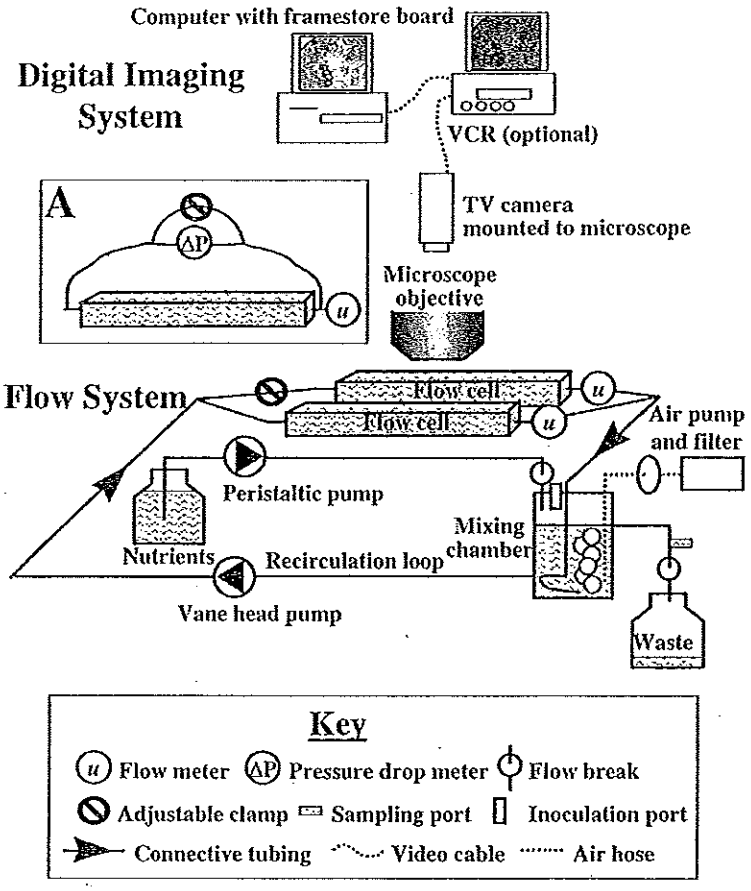

FIG. 1. Biofilm reactor system designed to image biofilms grown under laminar and turbulent flows. The schematic shows two parallel flow cells, although four have also been used. In our experiments we usually maintain laminar flow in one flow cell and turbulent flow in the other. The flow rate in the turbulent flow cell was controlled by the pump RPM and an adjustable clamp was used to reduce flow in the laminar flow cell. The inset "A" shows how the pressure drop meter was connected to the flow cell. A bypass loop facilitates flushing of air bubbles from the lines but must be clamped (as shown) during measurements.

system consists of either two or four parallel flow cells that are incorporated into a recycle loop with a mixing chamber for aeration and nutrient addition (Fig. 1). For flow cells we use 20 cm sections of square glass tubing (S-103 Camlab Ltd., Cambridge, U.K.) that are 3 mm wide (W) and 3 mm deep (D). The sections are cut from longer stock tubing with a diamond knife and the ends flame polished. Nutrients are delivered by peristaltic pump (Masterflex, Cole Parmer, Niles, IL) and the recycle flow rate is controlled with a vane head pump (Masterflex, Cole Parmer). Peristaltic pumps should be avoided because they provide a pulsatile flow in which there can be a wide range of shears. The volume (V) of the mixing chamber and recycle loop, including two flow cells, is approximately 175 ml. The nutrient influent flow rate (Q_n) is 4.3 ml/min, for a resulting residence time ($\theta = V/Q_n$) of

40 min. The flow rate through each of the flow cells (Q_f) is measured using flow meters (McMillan Flo-sensor model 101T # 3724 and 3835, supplied by Cole-Parmer). The flow meters are calibrated by timed volumetric displacement. To minimize disruption to the flow by sudden expansions and contractions in the recirculating loop, we use connective tubing (silicone or Phar-Med size 16, Cole-Parmer) and connectors with similar hydraulic diameters to the flow cells (3 mm). The tubing is connected directly to the flow cells and crimped using cable ties. To characterize the flow in the flow cells we measure the pressure drop (ΔP) across each flow cell (using differential pressure transducers RS Components, Corby, Northants, U.K., model 286-686) at different average flow velocities ($u_{(ave)} = Q_f/WD$). The pressure transducers are calibrated using a manometer. The flow velocity Q_f, through each flow cell can be controlled independently by tightening or loosening clamps on the inlet tubing. The flow cells are positioned on a polycarbonate holder that is mounted on the stage of an Olympus BH2 upright microscope with epifluorescence capabilities. The thickness of the glass wall of the flow cells limits observations to low numerical aperture long and ultralong working distance (LWD) objectives. However, 100 and 50× LWD objectives can resolve single cells on the top surface of the flow cells. To observe the biofilm growing on the bottom surface, objectives of 10× and lower are required to focus through the thickness of the entire flow cell. Under operating conditions the water temperature in the reactor system is 28° at a room temperature of 22°.

Hydrodynamic Characteristics of Flow Cells

We determined the hydrodynamic characteristics of the flow cells using the relationship between the Fanning friction factor (f) and Reynolds number (Re). The f and Re are found from ΔP, $u_{(ave)}$, and flow cell geometry. The Reynolds number (Re) is calculated from Eq. (1):

$$\mathrm{Re} = \frac{u_{(ave)} D_h}{\nu} \tag{1}$$

where D_h is the hydraulic diameter and ν is the kinematic viscosity. The D_h is (3 mm) from $D_h = 4\mathrm{CSA/WP}$ where CSA is the cross-sectional area ($\mathrm{CSA} = WD$) and WP the wetted perimeter ($\mathrm{WP} = 2W + 2D$) of the square flow cells. The f is found from[16] Eq. (2):

$$f = \frac{\Delta P \times D_h}{2 l_f \rho_w u_{(ave)}^2} \tag{2}$$

where ρ_w is the density of water and l_f is the distance between pressure ports. For ρ_w and ν we use values for water, since there is no significant difference between the

[16] W. G. Characklis, M. H. Turakhia, and N. Zelver, *in* "Biofilms" (W. G. Characklis and K. C. Marshall, eds.), p. 265. Wiley, New York, 1990.

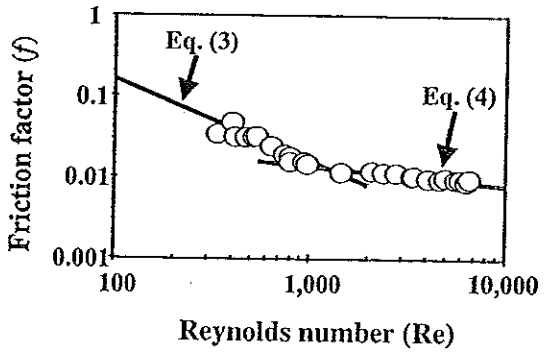

FIG. 2. Friction factor chart showing the measured (○) and predicted (—) values of f for a clean flow cell. The curve described by Eq. (3) shows the laminar region and Eq. (4) shows the turbulent region. The transition point occurred at approximately Re 1200.

viscosity (using a falling ball viscometer) of the sterile minimal salts medium[4,17] and distilled water ($p = 0.1, n = 6$), and the viscosity of the spent medium is only 1.2% greater than that of distilled water. Results show that the transition between laminar and turbulent flow occurs at Re 1200 ($u = 0.35$ m/sec) (Fig. 2). The measured f is in close agreement with that predicted by the Hagen–Poiseuille equation[18] in the laminar region:

$$f = \frac{16}{\mathrm{Re}} \tag{3}$$

and the Blasius formula[18] in the turbulent region:

$$f = 0.0791/\mathrm{Re}^{0.25} \tag{4}$$

for flow through smooth pipes. The transition point between flows occurs at a Re of approximately 1200. This has been confirmed by dye tracer studies.

In many experiments it is useful to report attachment or detachment of cells or microcolonies as a function of the wall shear stress caused by the moving fluid. In turbulent flow the shear stress at the wall (τ_w) can be estimated from[16,18] Eq. (5).

$$\tau_w = \frac{f\rho_w u_{(\mathrm{ave})}^2}{2} \tag{5}$$

In laminar flow:

$$\tau = \frac{4\eta u_{(\mathrm{max})}}{D_h} \tag{6}$$

where η is the absolute viscosity and $u_{(\mathrm{max})}$ is the maximum velocity. For a circular pipe $u_{(\mathrm{max})} = 2u_{(\mathrm{ave})}$ and for a flat plate reactor (when $W \approx 100D$) $u_{(\mathrm{max})}$ can be

[17] P. Stoodley, I. Dodds, J. D. Boyle, and H. M. Lappin-Scott, *J. Appl. Microbiol.* 85, 19S (1999).
[18] W. L. McCabe and J. C. Smith, "Unit Operations of Chemical Engineering," 3rd ed., Chemical Engineering Series. McGraw-Hill, New York, 1976.

approximated to $\frac{3}{2}u_{(ave)}$. However, for square flow cells the edge effects of the corners will cause τ_w to vary along the width of the wall, and Eqs. (5) and (6) will only give approximate estimates of τ_w. When correlating observed biofilm structure or dynamic phenomena with τ_w, images should be taken in the center area of the channel and the edges avoided. The shear distribution for laminar flow in square rectangular pipes can be calculated using analytical solutions described elsewhere.[19] However, these calculations are not trivial and there are no analytical solutions for turbulent flow. An alternative approach is to measure the velocity profile using particle image velocimetry[3] and calculate τ_w directly from Eq. (7):

$$\tau_w = \frac{\eta du}{dz} \tag{7}$$

where z is the distance from the wall; du/dz at the wall (i.e., when $z = 0$) can be determined graphically.

Reactor Sterilization

The reactor system and nutrients are sterilized by autoclaving at 121° for 15 min. The flow meters are sterilized using a method adapted from Fisher and Petrini[20] in which they are exposed to 70% ethanol for 15 min, 40% NaOCl solution (approximately 12% available chlorine when undiluted) for 15 min, and 70% ethanol for 15 min. The flow meters are then drained and positioned in the recycle loop aseptically by flame sterilized glass tubing connectors. When the pressure drop meters are used they are also sterilized by exposure to bleach and ethanol solutions. To check for sterility we operate the flow system with sterile media for 1 to 2 days prior to inoculation before plating three 0.1 ml effluent samples onto nutrient agar plates.

Image Capture and Analysis

A COHU 4612-5000 CCD camera (Cohu, Inc., San Diego, CA) is used to collect gray-scale images and a Scion VG-5 PCI framestore board (Scion Inc., Frederick, MD) is used for image capture. The framestore board is controlled with either NIH-Image (developed at the National Institutes of Health and available for free download at http://rsb.info.nih.gov/nih-image/) for use with a Macintosh or Scion Image (available at http://www.scioncorp.com/) for use with a PC. These software packages are also used for image enhancement and analysis. The VG-5 framestore board allows video rate imaging of 30 frames per second (fps). However, at this rate the computer RAM is quickly used up and we recommend at least 128 MB. It is also important to purchase a computer with adequate hard disk space for storage as well as having access to a CD writer or some other large-capacity

[19] F. M. White, "Viscous Fluid Flow," 2nd ed. McGraw-Hill, New York, 1991.
[20] P. J. Fisher and O. Petrini, *New Phytol.* **120,** 1370 (1992).

portable storage device such as Zip disks (Iomega, http://www.iomega.com/). Time lapse sequences are made by capturing images at programmed time intervals. Distance and area measurements are calibrated from pixels to microns using a 1 mm graticule with 10 μm divisions (Ref. # CS990, Graticules Ltd., Tonbridge, Kent, U.K.).

Application of Time Lapse Digital Imaging to Analyze Dynamic Behavior in Biofilms

Downstream Migration of Biofilm Ripples

A four species biofilm consisting of *Pseudomonas aeruginosa, P. fluorescens, Klebsiella pneumoniae,* and *Stenatrophomonas maltophilia* is grown in the previously described recirculating flow reactor[21] (Fig. 1) under turbulent flow of 1 m/sec. The biofilm is initially grown on a minimal salts medium (MSM) with 40 ppm glucose as the sole carbon source. After approximately 10 days the biofilm develops ripple-like structures on the walls of the flow cells. Low power (4 to 20× objectives) time-lapse images taken at 0.5 hr intervals over a 20 hr period have revealed that the biofilm appears to flow along the flow cells in a fluid-like manner as the ripples and other biofilm microcolonies migrate downstream along the walls of the flow cell (Figs. 3 and 4). The migration velocity is determined by measuring the location of individual ripples at different times (Fig. 4). We found the migration velocity is a function of the bulk liquid velocity and that the ripples have a maximum velocity of approximately 1 mm/hr when the bulk liquid velocity is approximately 0.5 m/sec. The time lapse images also revealed that, in some areas, ripples were continually detaching into the bulk liquid from the front (downstream edge) of the ripple bed, although it was not clear what initiated this detachment.[21]

Detachment of Biofilm Microcolonies

In a replicate set of experiments the four species biofilm was grown under turbulent flow for 21 days on MSM + 40 ppm glucose. The biofilm developed ripple structures similar to those observed in replicate experiments.[17] After 21 d the glucose concentration was increased to 400 ppm. Within 24 h the biofilm had increased in thickness from approximately 30 μm to 130 μm and the biofilm structure had markedly changed. The ripple structures had disappeared and the biofilm consisted of large oval shaped microcolonies separated by interstitial channels.[17] The structure was monitored for a further 2 days with no observed changes, and so it was assumed that the new structure was stable after this period. In this case low power time-lapse images did not show significant downstream motion but revealed

[21] P. Stoodley, Z. Lewandowski, J. D. Boyle, and H. M. Lappin-Scott, *Environ. Microbiol.* **1**, 447 (1999).

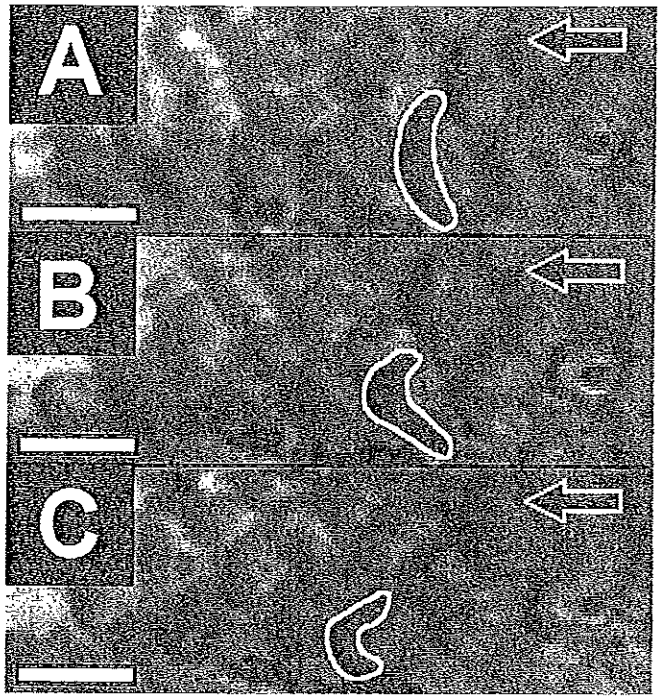

FIG. 3. Magnified region in a biofilm ripple bed showing an individual ripple (outlined in white) migrating downstream. The time interval between panels was 30 min. Scale bar = 80 μm. Note how the ripple changes shape as it moves along the surface.

that biofilm microcolonies were continually growing and detaching over a 20 hr monitoring period (Figs. 5 and 6). When each image was subtracted from the image taken previously using the "Image Math" routine in Scion Image (for settings we selected "real result" and set "x" at "1" and "+" at "0"), clusters that had detached appeared white. The image was then inverted and an appropriate threshold manually applied so that the clusters appeared black against a white background.

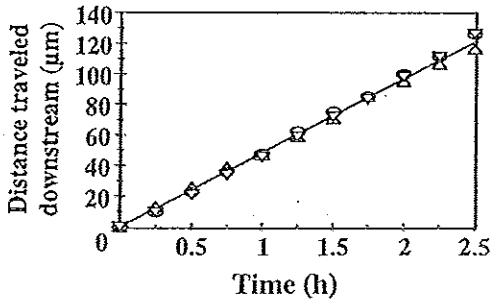

FIG. 4. The distance traveled downstream of three individual ripples in the ripple bed shown in Fig. 3 as a function of time. Over a 2.5 hr period the ripple velocity was a constant 49 μm/hr ($r^2 = 0.997$, $n = 33$) and there was very little variability between the velocity of the individual ripples.

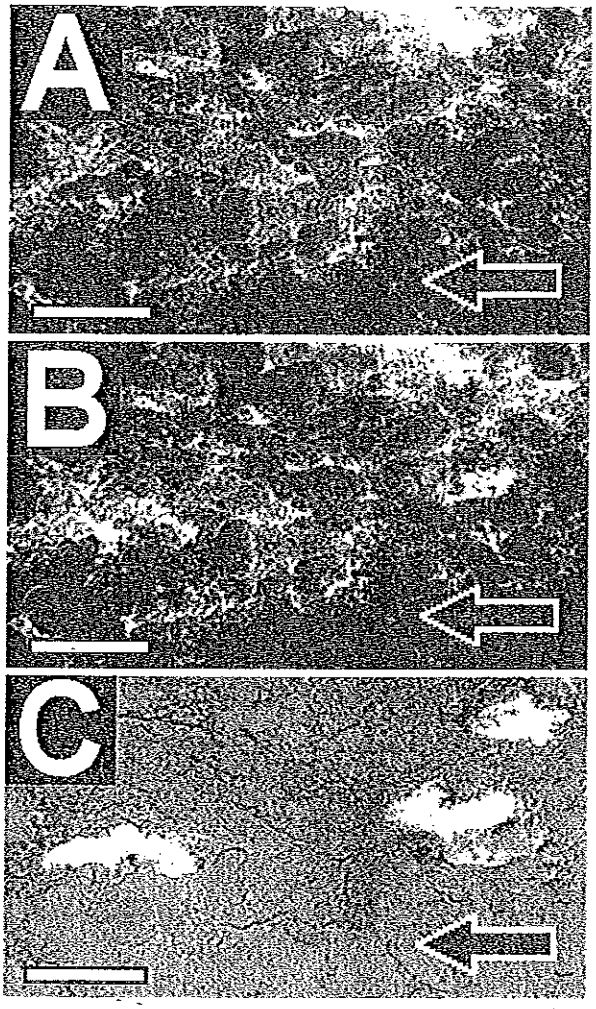

FIG. 5. Selected area from a larger field of view (area = 1.02 mm^2) showing the detachment of microcolonies from a 24 day old four species biofilm growing on MSM + 400 ppm glucose, Image "B" was subtracted from the image taken an hour earlier (A). Three large microcolonies that had detached during the elapsed time interval appeared as white areas on the resultant image "C." The direction of the bulk fluid flow is indicated by arrow. Scale bar = 200 μm.

The "Analyze Particles" routine was used to measure the number and area of clusters detaching between each time interval. These data can then be used to determine the detachment rate (Fig. 6) and the size distribution of detaching microcolonies.

Surface Area Coverage and Attachment of Microcolonies to a Surface

Mycobacterium fortuitum biofilms are grown on silastic or HDPE surfaces in a "once through" reactor system.[22] Since these experiments require surfaces

[22] L. Hall-Stoodley, C. W. Keevil, and H. M. Lappin-Scott, *J. Appl. Microbiol.* 85, S60 (1999).

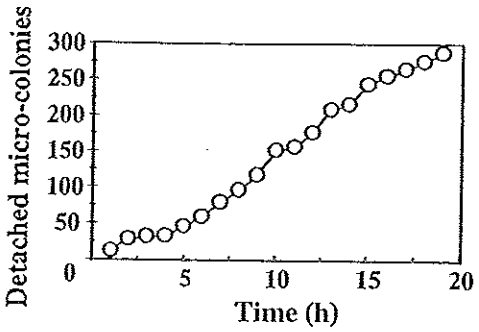

FIG. 6. The detachment rate of microcolonies from the area containing Fig. 5 was 14 mm^{-2} hr^{-1} ($r^2 = 0.96$, $n = 19$) calculated using the "Analyze Particles" routine on each subtracted image. The detachment rate was relatively constant over the 20 hr monitoring period. Because of limited resolution from the low power microscopy used (objective = 10×) only microcolonies with a projected area >140 μm (approx. diameter 14 μm) were included in the data set.

other than glass, we use a flat plate flow cell (BioSurface Technologies Corporation, http://www.imt.net/~mitbst/flowcell.html) with a recessed well in which coupons of different material can be fitted. The flow cell incorporates an overlying glass coverslip, for observing the developing biofilm. These flow cells allow the study of biofilm formation on a wide range of metallic and nonmetallic materials. However, they have the disadvantage that the channel depth is limited to 100 or 200 μm by the working distance of most high-resolution objectives. This in turn limits the flow regime to low, laminar flows. Also, because these types of flow cells generally have sudden expansions and contractions into and out of the coupon area, the hydrodynamics are often less well characterized. If the coupon is translucent, bright-field microscopy may be used for imaging, but reflected interference contrast or epifluorescence microscopy generally yield better images. Using this system with the same image analysis system as previously described, we have monitored the development and dynamic behavior of *M. fortuitum* biofilms. The progression of biofilm accumulation is monitored by measuring the percent surface area covered as a function of time. Images of the biofilm are captured using a low-power (20×) objective to increase the field area and give a better overall picture of the biofilm morphology. A threshold is then manually applied using the "Map" tool so the biofilm microcolonies appear black and the surrounding channels white. The total black area is recorded to a text file and the percent coverage calculated from the known field area. Single cells on the surface between the cell clusters cannot be observed at the low magnification and are therefore not included in the surface coverage measurement.

In addition to the routine monitoring of biofilm growth and accumulation, digital time lapse imaging is used to look for dynamic behavior in the biofilms. Although extensive ripple beds were not observed in these biofilms, some

FIG. 7. Attachment of *M. fortuitum* microcolonies to a silastic surface over a 1 hr interval. Image B was subtracted from the previous image (A). The individual cocci in the three outlined microcolonies that had attached during the 1-hr interval appeared black in the resultant image (C). Scale bar = 10 μm.

ripple-shaped and round microcolonies were seen moving over the surface in the downstream direction (unpublished results). Furthermore, image subtraction using "Image Math" showed that microcolonies up to 20 μm in length could reattach to the surfaces from the bulk liquid (Fig. 7). We estimated from these images that such microcolonies could each harbor on the order of several hundred cells. It is not yet known if such detached microcolonies have the antibiotic resistance often found in attached biofilms.

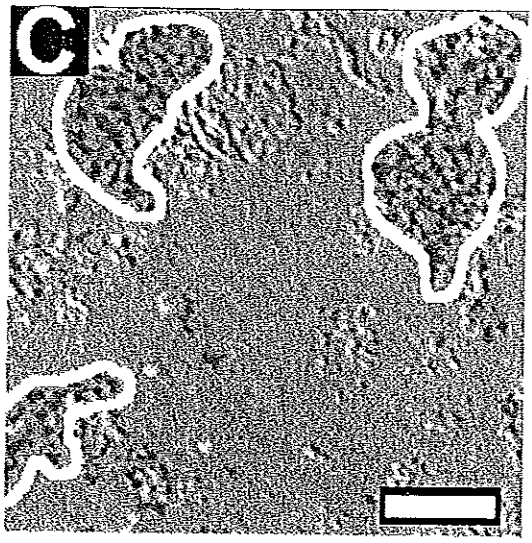

FIG. 7. (*continued*)

Conclusions

Digital time-lapse microscopic imaging by ourselves and others has revealed that biofilms not only are spatially complex but can also be temporally complex. Although this is more apparent during the initial stages of surface colonization, it can be more difficult to see in mature biofilms. It is often not evident that thicker, older biofilms are changing significantly, and an image taken one day may look very similar to an image taken on a different day. *In situ* microscopic measurements such as surface coverage and thickness, as well as scraping and conventional enumeration techniques used for monitoring biofilms, would indicate that the biofilm was in "steady state" with respect to biomass. However, with the use of time lapse imaging such dynamic process of growth, attachment, detachment, and motion of single cells and microcolonies can be observed and monitored. This work demonstrates that transient behavior in biofilms can cover a wide range of time scales, ranging from the high-frequency oscillations of biofilm filaments[23] to the slow surface migration of ripples,[21] which can be on the order of micrometers per hour. The notion of biofilms as dynamic, moving structural entities rather than static "coats of slime" has significant ramifications not only for how we view and model biofilms, but also as to how we may successfully control them. Furthermore, the detachment, reattachment, and movement of biofilm microcolonies over surfaces may give new insight into mechanisms by which infection or contamination may be disseminated in medical and industrial settings. As time lapse imaging continues to be used in the study of biofilms it is certain that other fascinating dynamic behavior will be revealed over a spectrum of time scales.

[23] P. Stoodley, Z. Lewandowski, J. Boyle, and H. M. Lappin-Scott, *Biotech. Bioeng.* 57, 536 (1998).

Acknowledgments

Work in the laboratories of P.S. and H.M.L.-S. was supported by grants from the National Institutes of Health (1 RO1 GM60052-01), the cooperative agreement EEC-8907039 between the National Science Foundation and Montana State University—Bozeman, and by the Wellcome Trust Ref. 050950/MJM/APH.